PHYSICAL REVIEW D **86,** 065002 (2012)

Chiral phase transition and critical end point in QED_3

Hongtao Feng,[1,*] Song Shi,[2] Peilin Yin,[2] and Hongshi Zong[2,3,†]

[1]*Department of Physics, Southeast University, Nanjing, People's Republic of China*
[2]*Department of Physics, Nanjing University, Nanjing, People's Republic of China*
[3]*Joint Center for Particle, Nuclear Physics and Cosmology, Nanjing 210093, China*

(Received 23 June 2012; published 5 September 2012)

In the framework of the truncated Dyson-Schwinger equation for the fermion propagator, we investigate the chiral and fermion number susceptibility at finite temperature and chemical potential in quantum electrodynamics in (2 + 1) dimensions (QED_3). The critical end point in the phase diagram of QED_3 is identified, and the behavior of these two susceptibilities around the critical end point is highlighted.

DOI: 10.1103/PhysRevD.86.065002 PACS numbers: 11.10.Kk, 11.15.Tk, 11.30.Qc

I. INTRODUCTION

A central goal of relativistic heavy ion collision experiments at RHIC, the LHC, and the future FAIR project is to chart the phase diagram of quantum chromodynamics (QCD) in the plane of temperature (T) and chemical potential (μ). This will provide fundamental insight into the origin of observable mass and the nature of the early Universe. Results with two massless quarks in QCD show that at high temperature, the phase transition associated to restoration of chiral symmetry is second-order and belongs to the universality class of $O(4)$ spin models in three dimensions [1]. Various results from QCD-inspired models (see, e.g., Refs. [2–5]) indicate that at low temperatures, the transition may be first-order for large values of the chemical potential. This suggests that the first-order transition line may end when the temperature increases. The phase diagram thus exhibits a critical end point (CEP) in the chiral limit, which separates the second-order transition line from the first-order one.

Due to the notorious sign problem, lattice Monte Carlo simulations cannot be used to do some direct computation at finite μ. Fortunately, nonperturbative tools not limited by the sign problem are at our disposal. In particular, it has been shown that Dyson-Schwinger equations (DSEs) is capable to describe the chiral transition at finite temperature and chemical potential [6]. Primarily, due to the complex non-Abelian structure of QCD, it is difficult to have a thorough understanding of chiral phase transition (CPT). In this case, to gain valuable insight into the relation between CPT and the order parameter for CPT before we can treat it completely, it is very suggestive to study some model which is similar to QCD and, at the same time, simpler. Since the discovery of high-T_c superconductivity, quantum electrodynamics in (2 + 1) dimensions (QED_3) has attracted more attention of the physicists. It is generally believed that QED_3 with N flavors can be regarded as a possible effective theory for high-T_c superconductivity in underdoped cuprates [7–9] and graphene [10,11]. Moreover, it has many features similar to QCD, for instance, dynamical chiral symmetry breaking [12–17] and confinement [18,19]. Therefore, it can serve as a toy model of QCD.

Then, a natural question may be raised: how to chart the chiral phase diagram of QED_3 at finite temperature and chemical potential and whether or not the phase diagram exhibits a CEP.

In recent years, some works in lattice QCD [20–22] showed that the peak of chiral susceptibility should be an essential characteristic of CPT. Later, based on techniques of continuum field theory, several groups [23–25] also gave the same conclusion. Meanwhile, in Ref. [26], the authors suggest that fermion-number susceptibility (FNS) should develop some singularity near the critical point. From then on, a lot of phenomenological model investigations as well as lattice simulations toward those susceptibilities have been attempted, all aimed at determining the location of the CEP on the (T-μ) plane [27,28]. Here it is interesting to use these two susceptibilities to investigate the phase diagram of QED_3 in the same framework and to see whether they yield results consistent with each other. The motivation of this paper is to adopt DSEs for the fermion propagator to study the behaviors of chiral and fermion number susceptibility at finite temperature and chemical potential and try to locate the CEP in QED_3.

II. CHIRAL SUSCEPTIBILITY

In Euclidean space, the Lagrangian of QED_3 at finite chemical potential reads

$$\mathcal{L} = \bar{\psi}(\not{\partial} + ie\not{A} - \gamma_3\mu + m)\psi + \frac{1}{4}F_{\sigma\nu}^2 + \frac{1}{2\xi}(\partial_\nu A_\nu)^2, \quad (1)$$

where the four-component spinors are employed and γ matrices satisfy the algebra $\{\gamma_\sigma, \gamma_\nu\} = \delta_{\sigma\nu}$. In the absence of the mass term $m\bar{\psi}\psi$, QED_3 has chiral symmetry.

There are several equivalent choices of the order parameter for chiral symmetry breaking; here, we use the fermion chiral condensate

*fenght@seu.edu.cn
†zonghs@chenwang.nju.edu.cn

$$\langle\bar{\psi}\psi\rangle_m = \int \frac{\mathrm{d}^3p}{(2\pi)^3}\,\mathrm{Tr}[S(m,p)], \tag{2}$$

where S is the dressed fermion propagator and Tr denotes trace over Dirac indices of the fermion propagator. Below, we shall determine the transition point via the maximum of the chiral susceptibility $\frac{\partial\langle\bar{\psi}\psi\rangle}{\partial m}$ (see, e.g., Refs. [23,28,29]), which is defined as [23]

$$\chi_a^c = \frac{\partial\langle\bar{\psi}\psi\rangle_m}{\partial m}\bigg|_{m\to 0}. \tag{3}$$

This equation indicates that the chiral susceptibility measures the response of the chiral condensate to an infinitesimal change of the fermion mass. Note, here, we evaluate chiral susceptibility in the chiral limit.

In order to derive a integral formula for the chiral susceptibility of QED_3 at finite temperature and density, let us first derive such a formula for the chiral susceptibility of QED_3 at zero temperature and density. Differentiating both sides of Eq. (2) with respect to m and using the identity

$$\frac{\partial S(m,p)}{\partial m} = -S(m,p)\frac{\partial S^{-1}(m,p)}{\partial m}S(m,p), \tag{4}$$

one arrives at

$$\chi_a^c = -\int \frac{\mathrm{d}^3p}{(2\pi)^3}\,\mathrm{Tr}[S(p)\Gamma(p)S(p)], \tag{5}$$

where the so-called scalar vertex $\Gamma(p) \equiv \frac{\partial S^{-1}(m,p)}{\partial m}|_{m\to 0}$. Therefore, we have obtained a closed integral formula which expresses the chiral susceptibility in terms of the dressed fermion propagator and the dressed scalar vertex, both of the latter objects being basic quantities in quantum field theory. The DSE approach provides a desirable framework to calculate these quantities and hence the chiral susceptibility.

Based on Lorentz structure analysis, the involved massive/massless fermion propagator at zero temperature and density can be written as

$$S^{-1}(m,p) = i\gamma\cdot pE(p^2) + F(p^2), \tag{6}$$

$$S^{-1}(p) \equiv S^{-1}(0,p) = i\gamma\cdot pA(p^2) + B(p^2). \tag{7}$$

In the high-energy limit, the fermion propagator reduces to the free one: $S_0^{-1}(p) = i\gamma\cdot p$. We suppose the inverse fermion propagator is analytic in the neighborhood of $m = 0$, and thus it can be Taylor expanded as

$$S^{-1}(m,p) = S^{-1}(p) + \frac{\partial S^{-1}(m,p)}{\partial m}\bigg|_{m\to 0} m + \cdots, \tag{8}$$

where the omitted terms are of high orders in m. In the limit $m \to 0$, these terms can be neglected, and the scalar vertex is written as

$$\begin{aligned}\Gamma(p) &\equiv \frac{\partial S^{-1}(m,p)}{\partial m}\bigg|_{m\to 0}\\ &= \left[\frac{i\gamma\cdot p\partial E(p^2)}{\partial m} + \frac{\partial F(p^2)}{\partial m}\right]_{m\to 0}\\ &\equiv i\gamma\cdot pC(p^2) + D(p^2).\end{aligned} \tag{9}$$

Substituting Eqs. (6) and (9) into Eq. (5), we obtain the general formula for the chiral susceptibility at zero temperature and density

$$\begin{aligned}\chi_a^c &= -\int \frac{\mathrm{d}^3p}{(2\pi)^3}\,\mathrm{Tr}\{S(p)[i\gamma\cdot pC(p^2) + D(p^2)]S(p)\}\\ &= 4\int \frac{\mathrm{d}^3p}{(2\pi)^3}\times\frac{A^2(p^2)D(p^2)p^2 - 2A(p^2)B(p^2)C(p^2)p^2 - B^2(p^2)D(p^2)}{[A^2(p^2)p^2 + B^2(p^2)]^2}.\end{aligned} \tag{10}$$

Here, we note that in the large momentum limit, $A(p^2)\to 1$, $B(p^2)\to 0$ and $D(p^2)\to 1$. From this, it can be seen that the integral in Eq. (10) is linearly divergent. In this case, we should employ a renormalization procedure to deal with this divergence. A natural approach is to subtract the chiral susceptibility of the free fermion field from the above chiral susceptibility. That is to say, we define the renormalized chiral susceptibility by

$$\chi^c \equiv \chi_a^c - \chi_f^c, \tag{11}$$

where χ_f^c is the chiral susceptibility of the free fermion gas. This renormalization is justified because this subtraction will never affect the general temperature and chemical potential effects of the chiral susceptibility which we are interested in. Based on Eqs. (10) and (11), we obtain the renormalized chiral susceptibility χ^c:

$$\begin{aligned}\chi^c &= \int \frac{\mathrm{d}^3p}{(2\pi)^3}\mathrm{Tr}[S_0(p)\mathbf{1}S_0(p) - S(p)\Gamma(p)S(p)]\\ &= 4\int \frac{\mathrm{d}^3p}{(2\pi)^3}\left\{\frac{A^2Dp^2 - 2ABCp^2 - B^2D}{[A^2p^2 + B^2]^2} - \frac{1}{p^2}\right\}.\end{aligned} \tag{12}$$

A. The dependence of χ^c on T and μ

Because the dressed fermion propagator plays an important role in charting the phase diagram of QED_3 at finite temperature and chemical potential, it is theoretically valuable to give a general recipe for calculating this function in the framework of the DSEs approach,

$$S^{-1}(m,p) = i\gamma\cdot p + m + \int \frac{d^3k}{(2\pi)^3}\gamma_\sigma S(m,k)\gamma_\nu D_{\sigma\nu}(m,q), \tag{13}$$

with $q = p - k$ and scale $e^2 = 1$ in this paper. Let us first recall the following general result given in Refs. [30,31]: If one ignores the μ dependence of the dressed photon propagator (this is a commonly used approximation in studying the dressed fermion propagator at finite μ [6,32,33]), then one can obtain the dressed fermion propagator at finite μ in a suitable truncation scheme from the one at $\mu = 0$ by the substitution

$$S^{-1}(m,\tilde{p}) = i\gamma\cdot\tilde{p}E(\tilde{p}^2) + F(\tilde{p}^2), \tag{14}$$

where $\tilde{p} = (P, p_3 + i\mu)$. Therefore, once the dressed fermion propagator at $\mu = T = 0$ is known, the dressed fermion propagator at finite μ and $T = 0$ can be obtained by means of Eq. (14). This result can be generalized to the case of finite temperature. The model fermion propagator at finite T and μ in this work can be taken to be the following form:

$$S^{-1}(m,\mu,T,P) = i\vec{\gamma}\,\vec{P}\,E_\parallel(\varpi_n,P^2) + i\varpi_n\gamma_3 E_3(\varpi_n,P^2) + F(\varpi_n,P^2), \tag{15}$$

where $\varpi_n = (2n+1)\pi T + i\mu$. Therefore, once the dressed fermion propagator at $\mu = T = 0$ is known, the dressed fermion propagator at finite μ and $T = 0$ can be obtained by means of Eqs. (13) and (15). Then, one can obtain the chiral susceptibility at finite temperature and chemical potential by replacing the integration over the third component of momentum with summation over fermion Matsubara frequencies in Eq. (12):

$$\begin{aligned}\chi^c(\mu,T) &= 4T\sum_n\int\frac{d^2P}{(2\pi)^2}\frac{\partial}{\partial m}\frac{F}{E_3^2\varpi_n^2 + E_\parallel^2P^2 + F^2}\Big|_{m\to 0} - \chi_f^c \\ &= 4T\sum_n\int\frac{d^2P}{(2\pi)^2}\times\left\{\frac{[A_3^2\varpi_n^2 + A_\parallel^2P^2 - B]D - 2A_3BC_3\varpi_n^2 - 2A_\parallel BC_\parallel P^2}{[A_3^2\varpi_n^2 + A_\parallel^2P^2 + B^2]^2} - \frac{1}{\varpi_n^2 + P^2}\right\},\end{aligned} \tag{16}$$

where $C_\parallel = \frac{\partial E_\parallel}{\partial m}|_{m\to 0}$, $C_3 = \frac{\partial E_3}{\partial m}|_{m\to 0}$.

B. Model for $\chi^c(\mu, T)$

In principle, the unknown functions in Eq. (16) can be obtained by solving the finite temperature and chemical potential version of the rainbow DSEs for the fermion propagator. Now, let us give a short review of previous studies on the effect of the wave-function renormalization factor $A_\parallel$ and A_3. At zero temperature, the results in Refs. [34–36], which are obtained in QED_3 with N fermion flavors, suggest that the $1/N$ order contribution from the vector function of fermion propagator only causes minor changes. Here, we also expect that leading order of DSE contribution plays the dominate role at finite temperature. So, we take the fermion renormalization constant $Z_{2=1}$ in this paper, and, hence, $A = E = 1$.

In order to obtain $S^{-1}(\mu, T, P)$ from Eq. (15), we employ a familiar boson propagator at finite temperature (we assume that it is μ-independent) [36–39],

$$D_{\sigma\nu}(m,T,Q) = \frac{\delta_{\sigma 3}\delta_{\nu 3}}{Q^2 + \Pi_0(m,T,Q)}. \tag{17}$$

Then, after some algebra, we obtain the corresponding DSE for the scalar function for the inverse massive fermion propagator in leading order:

$$\begin{aligned}F(P^2) &= m + T\sum_n\int\frac{d^2K}{(2\pi)^2}\frac{F(K^2)/[Q^2 + \Pi_0(m,T,Q)]}{\varpi_n^2 + K^2 + F(K^2)} \\ &= m + \int\frac{d^2K}{(2\pi)^2}\frac{F(K^2)(\tanh\frac{\mathcal{E}_k - \mu}{2T} + \tanh\frac{\mathcal{E}_k + \mu}{2T})}{4\mathcal{E}_k[Q^2 + \Pi_0(m,T,Q)]},\end{aligned} \tag{18}$$

with $\mathcal{E}_k = \sqrt{K^2 + F^2(K^2)}$. By application of some tricks (for more details, see the appendix), the zero-frequency boson polarization beyond the chiral limit can be reduced to

$$\Pi_0(m,T,Q) = \frac{T}{\pi}\int_0^1 dx\left\{\ln\left(4\cosh^2\frac{\sqrt{m^2 + x(1-x)Q^2}}{2T}\right) - \frac{m^2\tanh\frac{\sqrt{m^2+x(1-x)Q^2}}{2T}}{T\sqrt{m^2 + x(1-x)Q^2}}\right\}.$$

When $m \to 0$, the above function reduces to boson polarization in the chiral limit. With the general equation for the chiral susceptibility, we can obtain the chiral susceptibility at finite temperature and density in the leading order:

$$\chi^c(\mu,T) = 4T\int\frac{d^2P}{(2\pi)^2}\sum_n\left[\frac{D(P^2)}{\varpi_n^2+P^2+B^2(P^2)}-\frac{2D(P^2)B^2(P^2)}{[\varpi_n^2+P^2+B^2(P^2)]^2}-\frac{1}{\varpi_n^2+P^2}\right]$$
$$=\int\frac{d^2P}{(2\pi)^2}\left\{\frac{D(P^2)}{\mathcal{E}_p}\left(\tanh\frac{\mathcal{E}_p+\mu}{2T}+\tanh\frac{\mathcal{E}_p-\mu}{2T}\right)\left[1-\frac{B^2(P^2)}{\mathcal{E}_p^2}\right]+\frac{D(P^2)B^2(P^2)[\mathrm{sech}^2(\frac{\mathcal{E}_p+\mu}{2T})+\mathrm{sech}^2(\frac{\mathcal{E}_p-\mu}{2T})]}{2T\mathcal{E}_p^2}\right.$$
$$\left.-\frac{\tanh\frac{\sqrt{P^2}+\mu}{2T}+\tanh\frac{\sqrt{P^2}-\mu}{2T}}{\sqrt{P^2}}\right\}, \tag{19}$$

where the identities

$$\sum_n\frac{1}{\varpi_n^2+x^2}=\frac{\tanh\frac{x+\mu}{2T}+\tanh\frac{x-\mu}{2T}}{4xT},$$
$$\sum_n\frac{1}{[\varpi_n^2+x^2]^2}=\frac{\tanh\frac{x+\mu}{2T}+\tanh\frac{x-\mu}{2T}}{8Tx^3}-\frac{\mathrm{sech}^2\frac{x+\mu}{2T}+\mathrm{sech}^2\frac{x-\mu}{2T}}{16T^2x^2}$$

have been used. The unknown function in the above equation, $D(P^2)$, can be written as

$$D(P^2)=\frac{\partial F(P^2)}{\partial m}\bigg|_{m\to 0}. \tag{20}$$

An involved function in Eq. (20) is easily obtained

$$\Pi_0'(T,Q)=\frac{\partial\Pi_0(m,T,Q)}{\partial m}\bigg|_{m\to 0}=0,$$

and so Eq. (20) is written as

$$D(P^2)=1+\frac{1}{4}\int\frac{d^2K}{(2\pi)^2}\frac{D(K^2)}{\mathcal{E}_k[Q^2+\Pi_0(T,Q)]}\times\left\{\left(\tanh\frac{\mathcal{E}_k+\mu}{2T}+\tanh\frac{\mathcal{E}_k-\mu}{2T}\right)\left[1-\frac{B^2(K^2)}{\mathcal{E}_k^2}\right]+B^2(K^2)\left[\frac{\mathrm{sech}^2\frac{\mathcal{E}_k+\mu}{2T}+\mathrm{sech}^2\frac{\mathcal{E}_k-\mu}{2T}}{2T\mathcal{E}_k}\right]\right\}. \tag{21}$$

Then, from Eqs. (18), (19), and (21), we can obtain the chiral susceptibility at finite temperature and chemical potential in the leading order, and we also see that $\chi^c(\mu,T)$ depends linearly on the function $D(P^2)$. From those equations and Eq. (2) in the chiral limit, we can obtain the chiral susceptibility and chiral fermion condensate at finite T and μ.

C. Numerical results

To indicate the dependence of the susceptibility on T and μ, we shall first obtain the two involved functions B, D. Using iterative methods to resolve the coupled equations (18) at $m=0$ and (21) for a range of temperature and chemical potential, we can obtain the two scalar functions B, D. The typical behaviors of these two scalar functions are shown in Fig. 1. It is found that the value of these two functions decreases with the increasing momentum, and each reduces to a constant in the low-energy region.

The infrared values of $B(P^2)$ and $D(P^2)$ are shown in Fig. 2. As usual, $B(P^2)_{P^2\to 0}$ can be regarded as the order parameter for CPT, while $D(P^2)$ is related to the chiral susceptibility. Substituting these two functions into Eqs. (2) and (19), we immediately obtain the chiral fermion condensate and chiral susceptibility at finite T and μ. The dependence of the chiral condensate and susceptibility on the temperature for several chemical potentials are shown in Fig. 2.

The upper lines of Fig. 2 give the behavior of chiral susceptibility, while the lower lines in this figure show the behavior of the fermion chiral condensate. As is shown in Fig. 2, for any given chemical potential, χ^c almost keeps a constant at small temperature, while it shows an apparent peak at some critical temperature. This critical temperature depends on the chemical potential and diminishes as the chemical potential increases. From Fig. 2, it can also be seen that the fermion chiral condensate decreases as the temperature and chemical potential increase and vanishes when T reaches a critical value. This critical value also decreases with the increase of μ. Moreover, near the critical point of CPT, the susceptibility shows a large, actually divergent peak at small μ, while at high chemical potential, it is discontinuous and shows a finite peak. Compared with the two figures in Fig. 2, the vanishing self-energy brings out restoration of chiral symmetry, and

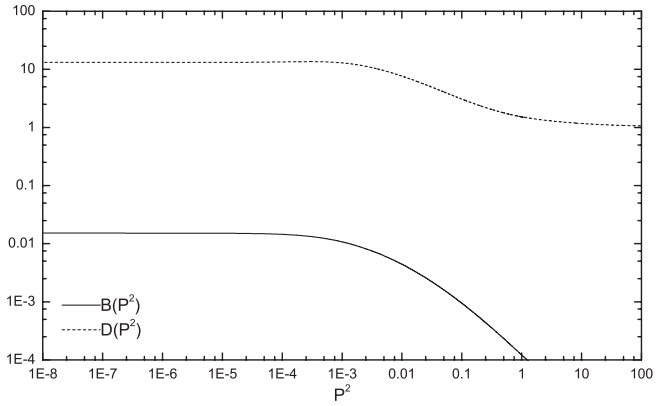

FIG. 1. The functions $B(P^2)$ and $D(P^2)$ in the chirally broken phase at $(T,\mu)=(10^{-3},10^{-2})$.

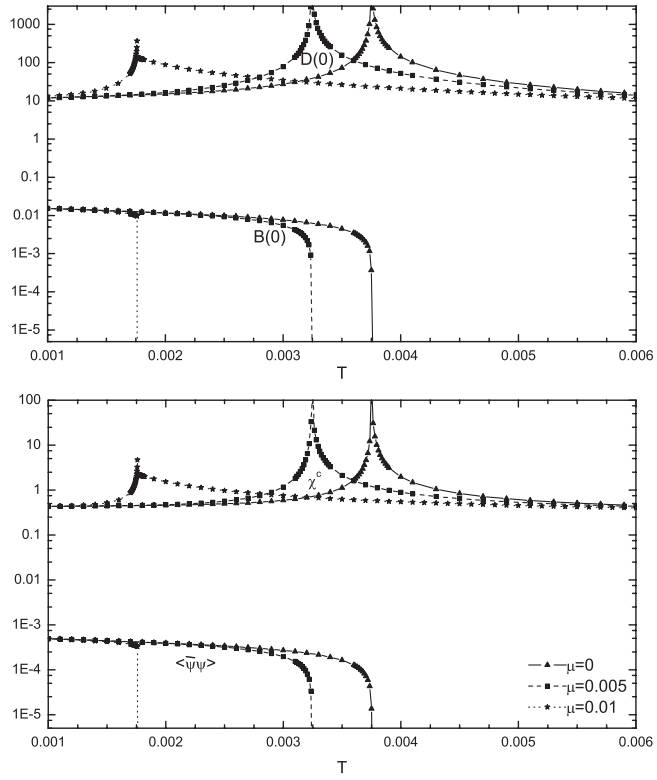

FIG. 2. The upper figure gives the infrared values of the functions $B(P^2)$ and $D(P^2)$ as functions of T with several μ; the lower one shows the dependence of chiral susceptibility and fermion chiral condensate on T and μ.

the divergent/finite peak of D corresponds to the divergent/finite susceptibility. It is also found that, for any chemical potential, the appearance of the peak of susceptibility and the disappearance of fermion chiral condensate occur at the same temperature.

III. FERMION NUMBER SUSCEPTIBILITY

The FNS is defined as the derivative of the fermion number density $\rho(\mu)$ with respect to the fermion chemical potential:

$$\chi_n = \frac{\partial \rho(\mu)}{\partial \mu}. \tag{22}$$

$\rho(\mu)$ can be expressed as (see, for example, Ref. [40]),

$$\rho(\mu) = -\int \frac{\mathrm{d}^3 p}{(2\pi)^3} \mathrm{Tr}[\hat{S}(\mu, p)\gamma_3], \tag{23}$$

where $\hat{S}(\mu, p)$ denotes the fermion propagator at finite μ. Using the identity

$$\frac{\partial \hat{S}(\mu, p)}{\partial \mu} = -\hat{S}(\mu, p)\frac{\partial \hat{S}^{-1}(\mu, p)}{\partial \mu}\hat{S}(\mu, p), \tag{24}$$

we can obtain

$$\chi_n = \int \frac{\mathrm{d}^3 p}{(2\pi)^3} \mathrm{Tr}\left[\hat{S}(\mu, p)\frac{\partial \hat{S}^{-1}(\mu, p)}{\partial \mu}\hat{S}(\mu, p)\gamma_3\right]. \tag{25}$$

Recall that the well-known Ward identity,

$$i\Gamma_\nu(0, p) = \frac{\partial S^{-1}(0, p)}{\partial p_\nu},$$

where p denotes the relative momentum of the vector vertex $\Gamma_\nu(0, p)$ and the corresponding total momentum vanishes. Then,

$$(-)\Gamma_3(0, p) = \frac{\partial \hat{S}^{-1}(\mu, p)}{\partial \mu}. \tag{26}$$

Substituting Eq. (26) into Eq. (25) and replacing the integration over the third component of momentum with explicit summation over Matsubara frequencies, we immediately arrive at the general expression for FNS at finite temperature and density:

$$\chi_n(\mu, T) = -T\sum_n \int \frac{\mathrm{d}^2 P}{(2\pi)^2} \mathrm{Tr}[\hat{S}(\tilde{p})\Gamma_3(0, \tilde{p})\hat{S}(\tilde{p})\gamma_3]. \tag{27}$$

The above model-independent integral formula for the FNS is totally determined by the third component of the dressed vector fermion-boson vertex and the fermion propagator. Naturally, the next step is to calculate the latter two objects. Here, we also employ DSEs to resolve these quantities and then investigate the fermion-number susceptibility.

A. Free fermion-number susceptibility

Before going to the model calculation of FNS, let us analyze the limiting behavior of FNS at high temperature and density. In the limit of high temperature and density, the dressed fermion propagator reduces to the free one,

$$\hat{S}^{-1}(\mu, p) = i\gamma \cdot \tilde{p}, \tag{28}$$

and the corresponding vertex reduces to

$$\Gamma_3(0, \tilde{p}) = \gamma_3. \tag{29}$$

Inputting Eqs. (28) and (29) into Eq. (27), we obtain the free FNS

$$\begin{aligned}
\chi_n^f &= -T\sum_n \int \frac{\mathrm{d}^2 P}{(2\pi)^2} \mathrm{Tr}\left[\frac{1}{i\gamma\tilde{p}}\gamma_3\frac{1}{i\gamma\tilde{p}}\gamma_3\right] \\
&= 4T\int \frac{\mathrm{d}^2 P}{(2\pi)^2} \times \sum_n \left[\frac{1}{\varpi_n^2 + \mathcal{E}_{p0}^2} - \frac{2\mathcal{E}_{p0}^2}{[\varpi_n^2 + \mathcal{E}_{p0}^2]^2}\right] \\
&= 2\beta\int \frac{\mathrm{d}^2 P}{(2\pi)^2}\left\{\frac{e^{\beta(\mathcal{E}_{p0}+\mu)}}{[e^{\beta(\mathcal{E}_{p0}+\mu)}+1]^2} + \frac{e^{\beta(\mathcal{E}_{p0}-\mu)}}{[e^{\beta(\mathcal{E}_{p0}-\mu)}+1]^2}\right\} \\
&= 2\frac{\partial}{\partial\mu}\int \frac{\mathrm{d}^2 P}{(2\pi)^2}\left\{\frac{1}{e^{\beta(\mathcal{E}_{p0}-\mu)}+1} - \frac{1}{e^{\beta(\mathcal{E}_{p0}+\mu)}+1}\right\} \\
&= \frac{T}{\pi}\ln(e^{\beta\mu} + e^{-\beta\mu} + 2),
\end{aligned} \tag{30}$$

where $\mathcal{E}_{p0} = \sqrt{P^2}$, $\beta = 1/T$. From Eq. (30), it can be seen that the limiting value of χ_n^f at zero temperature and finite density, and the one at zero density and finite temperature, are

$$\lim_{T\to 0}\chi_n^f = \frac{\mu}{\pi}, \qquad \lim_{\mu\to 0}\chi_n^f = \frac{T}{\pi}\ln 4, \tag{31}$$

respectively.

B. Model for the susceptibility

To calculate the FNS, we have to calculate the dressed fermion propagator and dressed vector vertex at finite temperature and chemical potential in advance. The integral equation for the dynamically generated fermion self-energy function at finite temperature can be written as

$$\begin{aligned} B(P^2) &= T\sum_n \int \frac{\mathrm{d}^2K}{(2\pi)^2}\frac{B(K^2)/[Q^2 + \Pi_0(T,Q)]}{\varpi_n^2 + K^2 + B^2(K^2)} \\ &= \int \frac{\mathrm{d}^2K}{(2\pi)^2}\frac{B(K^2)[\tanh\frac{\mathcal{E}_k-\mu}{2T} + \tanh\frac{\mathcal{E}_k+\mu}{2T}]}{4\mathcal{E}_k[Q^2 + \Pi_0(T,Q)]}, \end{aligned} \tag{32}$$

where $\mathcal{E}_k = \sqrt{K^2 + B^2(K^2)}$ and the Matsubara frequency has been summed analytically. Of course, the fermion self-energy depends on the temperature and chemical potential. The boson polarization is given in Refs. [34,37],

$$\Pi_0(T,Q) = \frac{1}{8}\left[Q + T\frac{16\ln 2}{\pi}\exp\left(-\frac{\pi Q}{16T\ln 2}\right)\right]. \tag{33}$$

Following the above approximation, we take $\Gamma_3 \to \gamma_3$ and then the particle-number susceptibility reduces to

$$\chi_n = 2\beta\int\frac{\mathrm{d}^2P}{(2\pi)^2}\left\{\frac{e^{\beta(\mathcal{E}_p+\mu)}}{[e^{\beta(\mathcal{E}_p+\mu)}+1]^2} + \frac{e^{\beta(\mathcal{E}_p-\mu)}}{[e^{\beta(\mathcal{E}_p-\mu)}+1]^2}\right\}. \tag{34}$$

After the fermion self-energy is obtained, one can calculate the fermion chiral condensate and FNS.

C. Numerical results

Substituting Eq. (32) into Eqs. (2) and (34), we also obtain the chiral fermion condensate and fermion number susceptibility at finite T and μ. The typical dependence of FNS on the temperature for several values of chemical potential are shown in Fig. 3. The upper figure in Fig. 3 shows the behavior of fermion chiral condensate, while the lower figure in Fig. 3 shows the behavior of FNS, where $\chi(\mu, T)$ is normalized by the FNS in the case of free fermion gas χ_n^f (33) and is hence dimensionless.

Let us analyze the observations from this figure. As is shown in Fig. 3, for any given chemical potential, χ rises with the increasing temperature and shows an apparent inflexion and then $\chi = 1$ beyond a critical temperature $T_c(\mu)$. This critical temperature depends on the chemical potential and diminishes as the chemical potential

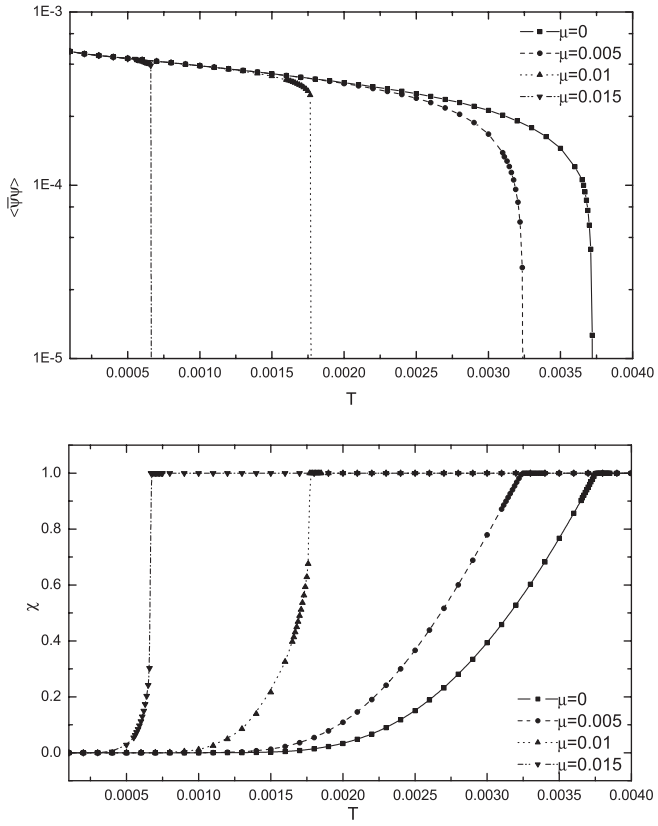

FIG. 3. The dependence of $\langle\bar{\psi}\psi\rangle$ (up) and $\chi = \chi_n/\chi_n^f$ (down) on the temperature for several values of μ.

increases. From Fig. 3, it can also be seen that the fermion chiral condensate decreases as the temperature and chemical potential increase and vanishes when T reaches a critical value. This critical value also decreases with the increasing of μ. Comparing with the two figures, we see that the vanishing fermion chiral condensate brings out restoration of chiral symmetry and corresponds to the clockwise inflexion of $\chi(\mu, T)$. That is to say, for any given chemical potential, the appearance of the inflexion of susceptibility and the disappearance of fermion chiral condensate occur at the same temperature.

IV. PHASE DIAGRAM

Now, we are in a position to study the phase diagram of QED_3 by analyzing the temperature and density dependence of these two susceptibilities. First, let us see the chiral susceptibility. When the chemical potential is small, the susceptibility gives a large and acutely divergent value. As the chemical potential increases and reaches a critical value μ_e, the chiral susceptibility remains discontinuous, but the corresponding peak has a finite value near the point of CPT. The critical temperature and chemical potential of the fermion chiral condensate and the susceptibility are plotted in Fig. 4. Two separate phases are shown in the T-μ plane: the chiral symmetry restored phase and the phase

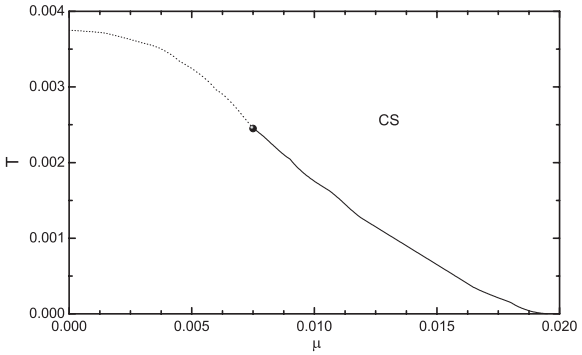

FIG. 4. The phase diagram for the condensate and susceptibility. The solid line represents the first-order transition, and the dotted line gives the second-order transition. The black circle indicates the position for CEP in the Lagrangian (1).

with chiral symmetry dynamically broken. The solid line represents discontinuous chiral susceptibility, and the chiral susceptibility shows a finite peak, which begins from $\mu_c = 0.0195$ at vanishing temperature and ends at the end point ($T_e = 2.45 \times 10^{-3}$, $\mu_e = 7.5 \times 10^{-3}$). Beyond T_e, one ends up with divergent susceptibility (dotted line) to a so-called pseudocritical temperature $T_c = 3.75 \times 10^{-3}$ at vanishing chemical potential.

Now, let us see the case of FNS. Around (T_e, μ_e), FNS shows different behaviors from the chiral susceptibility. When the chemical potential is small, the susceptibility exhibits a continuous rise near the chiral critical temperature, which is a typical characteristic of continuous phase transition. However, as the chemical potential increases and reaches a critical value which is the same as μ_e, the susceptibility exhibits a skip across $T_c(\mu)$ and has a discontinuity due to its first-order phase transition character. We plot the critical temperature and critical chemical potential for the FNS in Fig. 4 (here, the phase diagrams extracted from the critical behaviors of FNS and chiral susceptibility are the same, so we plot it in one figure). As is shown in Fig. 4, two separate phases exist in the T-μ plane: chiral symmetry and the phase with dynamical chiral symmetry breaking. In Fig. 4, the solid line represents the skip of the susceptibility, which begins from 1.95×10^{-2} at vanishing temperature and ends at the CEP which also lies at (T_e, μ_e). Below μ_e, the susceptibility reveals a continuous rise (represented by the dotted line). This line extends to $T_c = 3.75 \times 10^{-3}$ at vanishing chemical potential.

In this paper, we try to study two different susceptibilities of QED_3, i.e., the FNS and chiral susceptibility, and from these we extract the phase diagram of QED_3 in the (T-μ) plane. By comparing the behaviors of FNS and chiral susceptibility we find that they give the same phase diagram. This is what one expects in advance since these two order parameters should give the same physical results. From Fig. 4, it can be seen that near the critical point of CPT, chiral susceptibility is discontinuous and shows a finite peak, while the FNS shows a skipping behavior. This shows that at high density, it is a first-order phase transition (the solid line). While at high temperature, a divergent chiral susceptibility corresponds to a continuous FNS, which shows it is a second order phase transition (the dotted line). This suggests that both FNS and chiral susceptibility can be regarded as equivalent order parameters for studying chiral phase transitions in QED_3.

V. CONCLUSIONS

The primary goal of this paper is to identify and locate the CEP in QED_3 through a continuum study of the quark number and chiral susceptibility. To this end, we first derive a model-independent integral formula expressing the chiral and quark number susceptibility in terms of dressed fermion propagator and the corresponding dressed vertex. Then, based on the suitable approximation of truncated DSEs for the fermion propagator and numerical model calculations, we study the behavior of FNS and chiral susceptibility near the critical point of CPT in QED_3. We find that, with the rise of temperature and chemical potential, the appearance of the peak of chiral susceptibility and CPT occur at the same critical point. At the critical point, the curve of FNS shows an inflexion.

Moreover, we find that both of these two order parameters exhibit different behaviors at the chiral-phase transition point. Our calculation predicts that the CEP lies at (T_e, μ_e). Around this point, the peak of chiral susceptibility is divergent, and FNS shows a continuous behavior at high temperature, which exhibits a typical characteristic of second-order phase transition driven by chiral symmetry restoration. Nevertheless, at high density, chiral susceptibility is discontinuous and has a finite peak, while FNS jumps. This is a typical first-order phase transition. From this, we obtain the phase diagram of QED_3 in the (T-μ) plane.

The model we have used in the present work is of course schematic and might be far from reality (for example, we have neglected the effect of the wave-function renormalization factor A and C [13,17,36,37,41]). We note, however, that this is the first time which one observes CEP in QED_3, which is similar to the case of QCD [4,27,28,42]. In order to further confirm this observation, we need to study this problem in more realistic models.

ACKNOWLEDGMENTS

We would like to thank Dr. Yu Jiang and Professor Wei-Min Sun for helpful discussions. This work was supported by the National Natural Science Foundation of China (under Grant Nos. 11047005, 11105029, 10935001 and 11075075) and a project funded by the Priority Academic Program Development of Jiangsu Higher Education Institution.

APPENDIX A: BOSON POLARIZATION WITH FINITE FERMION MASS AT $T \neq 0$

Beyond the chiral limit, the boson polarization tensor in one-loop order at zero temperature and zero density reads

$$\Pi_{\sigma\nu}(m,q) = -\alpha \int \frac{d^3k}{(2\pi)^3} \mathrm{Tr}\left[\frac{\gamma_\sigma(m - i\not{k})\gamma_\nu(m - i\not{p})}{(k^2+m^2)(p^2+m^2)}\right]$$
$$= 4\alpha \int \frac{d^3k}{(2\pi)^3} \times \left[\frac{k_\sigma p_\nu + k_\nu p_\sigma - (pk+m^2)\delta_{\sigma\nu}}{(k^2+m^2)(p^2+m^2)}\right],$$

where $q = p - k$ and $\alpha = e^2$. Setting $l = k + qx$, we can write the above equation as

$$\Pi^{m'}_{\sigma\nu} = 4\alpha \int \frac{d^3k}{(2\pi)^3} \int_0^1 dx \frac{I_{\sigma\nu}}{[l^2 + x(1-x)q^2 + m^2]^2}, \tag{A1}$$

where

$$I_{\sigma\nu} = 2x(1-x)(q^2\delta_{\sigma\nu} - q_\sigma q_\nu) - [l^2 + x(1-x)q^2 + m^2]\delta_{\sigma\nu} + 2l_\sigma l_\nu + (1-2x)(l_\sigma q_\nu + l_\nu q_\sigma - lq\delta_{\sigma\nu}). \tag{A2}$$

At finite temperature, $l = (l_0, L)$, $l_0 = 2(n + xm' + \frac{1}{2})\pi T$. Following the approximation in the chiral limit [38], we also keep the zero-frequency value of the polarization ($q_0 = 0$) and then arrive at

$$\Pi_{00}(Q,T) = 4T\alpha \int \frac{d^2L}{(2\pi)^2} \int_0^1 dx \sum_n \times \left[\frac{1}{l_0^2 + L^2 + x(1-x)q^2 + m^2} - \frac{2[L^2 + m^2 + x(1-x)q_0^2] - (1-2x)l_0q_0}{[l_0^2 + L^2 + x(1-x)q^2 + m^2]^2}\right]$$
$$= \frac{2T\alpha}{\pi} \int_0^1 dx \int_{\frac{C}{2T}}^\infty dz \times \left[\frac{x(1-x)q^2}{4T^2}\left(\frac{\tanh z}{z^2} - \frac{\mathrm{sech}^2 z}{z}\right) + z \cdot \mathrm{sech}^2 z\right],$$

where $C^2 = m^2 + x(1-x)q^2$, $z = \frac{\sqrt{L^2+C^2}}{2T}$ and the following formulas

$$\int_A^\infty dz z \cdot \mathrm{sech}^2 z = \ln(2\cosh A) - A\tanh A, \qquad \int_A^\infty dz\left(\frac{\tanh z}{z^2} - \frac{\mathrm{sech}^2 z}{z}\right) = \frac{\tanh A}{A},$$

are used. Finally, the boson polarization with zero-frequency approximation at finite temperature is obtained:

$$\Pi^0_{00}(m,T,Q) = \frac{T\alpha}{\pi} \int_0^1 dx \left\{\ln\left(4\cosh^2 \frac{\sqrt{m^2 + x(1-x)Q^2}}{2T}\right) - \frac{m^2 \tanh\frac{\sqrt{m^2+x(1-x)Q^2}}{2T}}{T\sqrt{m^2 + x(1-x)Q^2}}\right\}.$$

[1] K. Rajagopal, Nucl. Phys. **A661**, 150 (1999).
[2] M. A. Stephanov, Phys. Rev. Lett. **76**, 4472 (1996).
[3] A. Barducci, R. Casalbuoni, S. De Curtis, R. Gatto, and G. Pettini, Phys. Rev. D **41**, 1610 (1990).
[4] S. X. Qin, L. Chang, H. Chen, Y. X. Liu, and C. D. Roberts, Phys. Rev. Lett. **106**, 172301 (2011).
[5] Y. Jiang, H. Gong, W. M. Sun, and H. S. Zong, Phys. Rev. D **85**, 034031 (2012).
[6] C. D. Roberts and S. M. Schmidt, Prog. Part. Nucl. Phys. **45**, S1 (2000).
[7] I. F. Herbut and B. H. Seradjeh, Phys. Rev. Lett. **91**, 171601 (2003).
[8] M. Franz, Z. Tesanovic, and O. Vafek, Phys. Rev. B **66**, 054535 (2002).
[9] G. Z. Liu, Phys. Rev. B **71**, 172501 (2005).
[10] K. S. Novoselov, A. K. Geim, S. V. Morozov, D. Jiang, M. I. Katsnelson, I. V. Grigorieva, S. V. Dubonos, and A. A. Firsov, Nature (London) **438**, 197 (2005).
[11] V. P. Gusynin, S. G. Sharapov, and J. P. Carbotte, Int. J. Mod. Phys. B **21**, 4611 (2007).
[12] G. Z. Liu and G. Cheng, Phys. Rev. D **67**, 065010 (2003).
[13] T. Appelquist, D. Nash, and L. C. R. Wijewardhana, Phys. Rev. Lett. **60**, 2575 (1988).
[14] D. Nash, Phys. Rev. Lett. **62**, 3024 (1989).
[15] R. D. Pisarski, Phys. Rev. D **29**, 2423 (1984).
[16] H. T. Feng, F. Hu, W. M. Sun, and H. S. Zong, Commun. Theor. Phys. **43**, 501 (2005).
[17] P. Maris, Phys. Rev. D **54**, 4049 (1996).
[18] C. J. Burden, J. Praschifka, and C. D. Roberts, Phys. Rev. D **46**, 2695 (1992).
[19] P. Maris, Phys. Rev. D **52**, 6087 (1995).
[20] F. Karsch and E. Laermann, Phys. Rev. D **50**, 6954 (1994).
[21] M. Cheng *et al.*, Phys. Rev. D **75**, 034506 (2007).
[22] L. K. Wu, X. Q. Luo, and H. S. Chen, Phys. Rev. D **76**, 034505 (2007).
[23] M. He, Y. Jiang, W. M. Sun, and H. S. Zong, Phys. Rev. D **77**, 076008 (2008).
[24] L. Chang, Y. X. Liu, C. D. Roberts, Y. M. Shi, W. M. Sun, and H. S. Zong, Phys. Rev. C **79**, 035209 (2009).
[25] M. He, F. Hu, W. M. Sun, and H. S. Zong, Phys. Lett. B **675**, 32 (2009).
[26] M. Stephanov, K. Rajagopal, and E. Shuryak, Phys. Rev. Lett. **81**, 4816 (1998); Phys. Rev. D **60**, 114028 (1999).

[27] M. He, J. F. Li, W. M. Sun, and H. S. Zong, Phys. Rev. D **79**, 036001 (2009).
[28] C. S. Fisher, J. Luecker, and J. A. Muller, Phys. Lett. B **702**, 438 (2011).
[29] F. Karsch and E. Laermann, Phys. Rev. D **50**, 6954 (1994).
[30] H. T. Feng, F. Y. Hou, X. He, W. M. Sun, and H. S. Zong, Phys. Rev. D **73**, 016004 (2006).
[31] H. T. Feng, D. K. He, W. M. Sun, and H. S. Zong, Phys. Lett. B **661**, 57 (2008).
[32] H. S. Zong, L. Chang, F. Y. Hou, W. M. Sun, and Y. X. Liu, Phys. Rev. C **71**, 015205 (2005).
[33] F. Y. Hou, L. Chang, W. M. Sun, H. S. Zong, and Y. X. Liu, Phys. Rev. C **72**, 034901 (2005).
[34] I. J. R. Aitchison and M. Klein-Kreisler, Phys. Rev. D **50**, 1068 (1994).
[35] M. He, H. T. Feng, W. M. Sun, and H. S. Zong, Mod. Phys. Lett. A **22**, 449 (2007).
[36] I. J. R. Atichison, N. Dorey, M. Klein-Kreisler, and N. E. Mavromatos, Phys. Lett. B **294**, 91 (1992).
[37] N. Dorey and N. E. Mavromatos, Phys. Lett. B **266**, 163 (1991).
[38] N. Dorey and N. E. Mavromatos, Nucl. Phys. **B386**, 614 (1992).
[39] J. F. Li, Y. Q. Zhou, H. T. Feng, W. M. Sun, and H. S. Zong, Mod. Phys. Lett. A **25**, 2645 (2010).
[40] H. T. Feng, M. He, W. M. Sun, and H. S. Zong, Phys. Lett. B **688**, 178 (2010).
[41] C. S. Fischer, R. Alkofer, T. Dahm, and P. Maris, Phys. Rev. D **70**, 073007 (2004).
[42] R. V. Gavai and S. Gupta, Phys. Rev. D **71**, 114014 (2005).